THz-frequency magnetic resonance

Marcin Białek[1]

[1] Institute of Physics, École Polytechnique Fédérale de Lausanne (EPFL), 1015 Lausanne, Switzerland

Towards Terahertz Technology for High Throughput Communications
Lausanne, Switzerland, 6th of February 2020

Head of the group:
prof. Jean-Philippe Ansermet
THz part of our group:
Jianyu Zhang (Beihang University, Beijing)
samples:
dr. Arnaud Magrez, dr. Toshimitsu Ito (AIST, Japan), prof. Anhua Wu (Shaghai Insitute of Ceramics)
EPR, NMR, DNP and electrochemistry:
dr. Mika Tamski, dr. Jonas Milani, dr. Soundarajian Murari, dr. Dongyoon Yoon
equipment:
Virginia Diodes extenders and boards, Swissto12 quasioptical elements

Outline

Gap Crossover of laboratory THz technologies

Band of frequencies at a crossover of techniques based on optical sources and those based on electronics.

- Optical side starts at about 0.1 THz (TDS).
- Frequency extenders for VNA can reach up to 1.5 THz.

However, the THz gap still exists in applications.

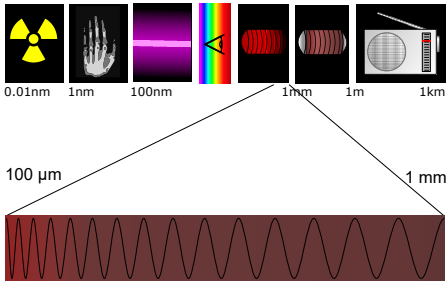

[1] image source: Wikipedia, CC-BY-SA

Electron paramagnetic resonance

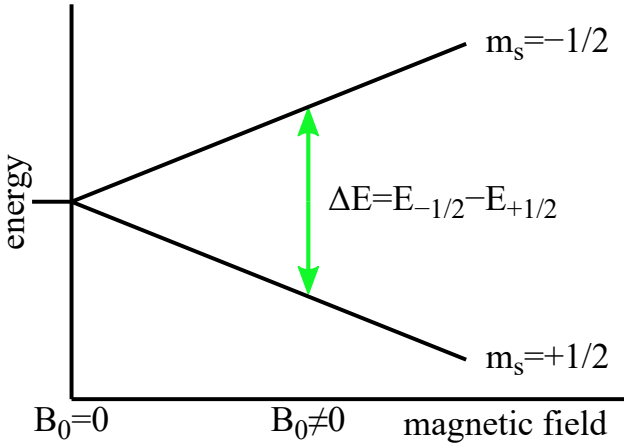

$\Delta E = g_s \mu_B B_0$

$\omega = \gamma B_0$

$\gamma/2\pi = 28.0$ GHz/T

Electron paramagnetic resonance

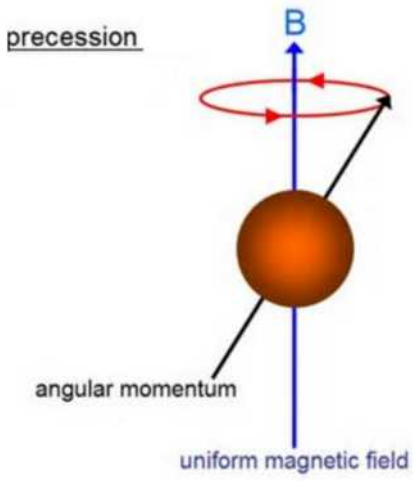

$$\frac{d\mu}{dt} = \gamma\mu \times \mathbf{B}$$
$$\omega = \gamma B_0$$

High-field electron paramagnetic resonance

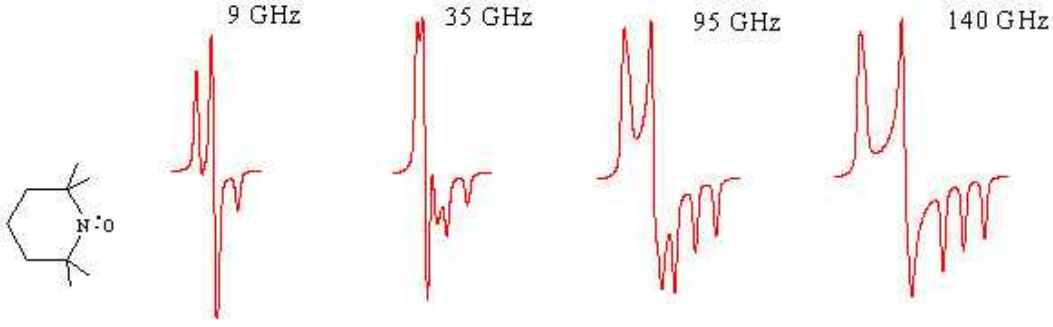

High-field EPR at EPFL

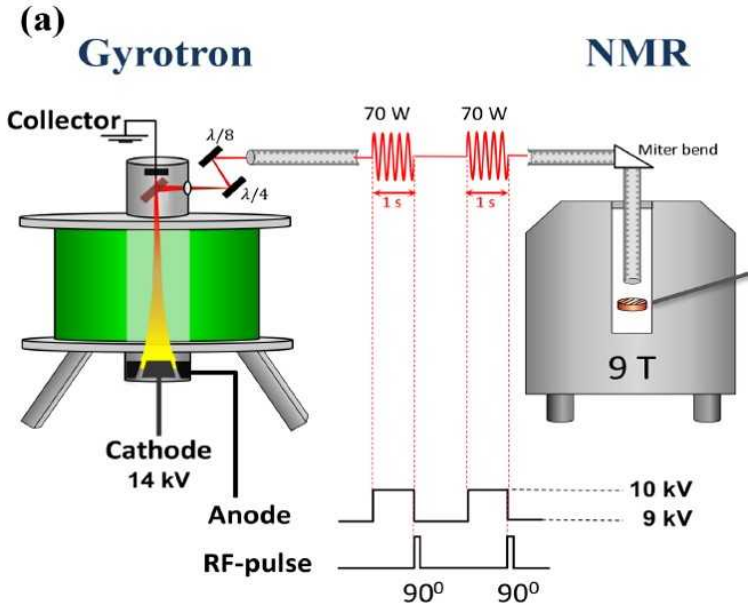

High-field EPR at EPFL

Swissto12
terahertz applications

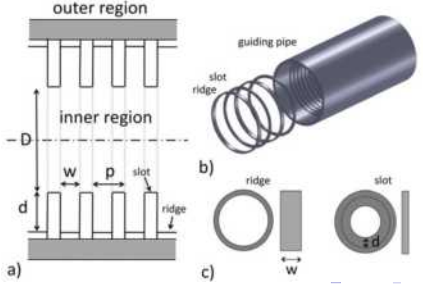

High-field EPR at EPFL

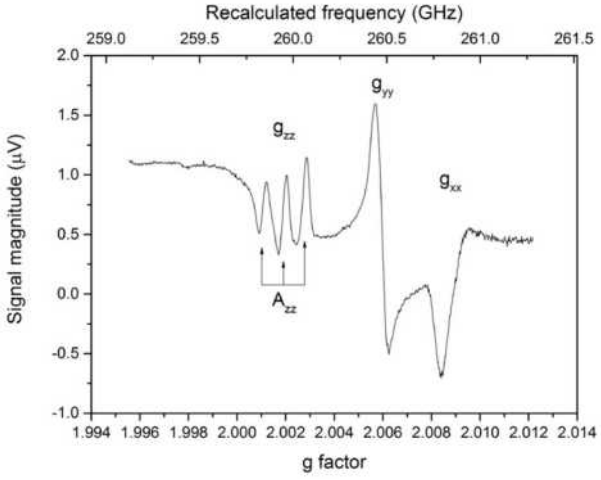

frozen solution of TEMPOL

Frequency extenders to vector network analyzer (VNA)

- Very high dynamic range (120 dB), stability and frequency resolution.
- VNA signals are multiplied at nonlinear elements.
- Antenna emits free beam of radiation.

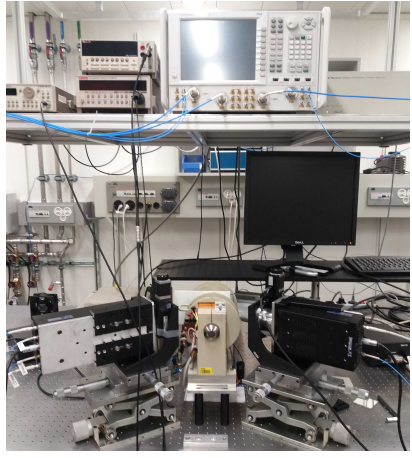

Ferromagnetic resonance

$\frac{d\mathbf{M}}{dt} = \gamma \boldsymbol{M} \times \mathbf{B}$

$\omega = \gamma \sqrt{B_0(B_0 + \mu_0 M)}$

$\mu_0 M = \chi B_0$ ..., but hysteresis

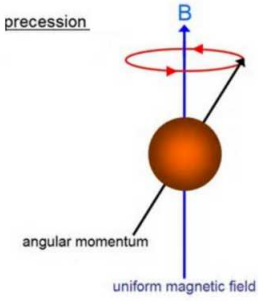

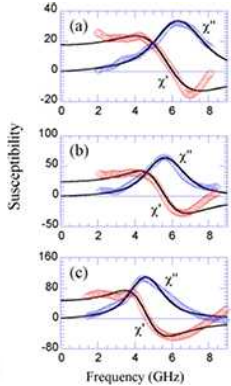

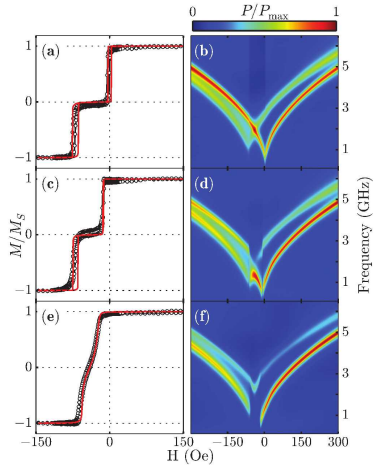

[1] Vergara et al., J. Phys. D: Appl. Phys. **48** 435003 (2015)

[2] Gonzalez-Chavez et al., Phys. Rev. B **88** 104431 (2013)

Ferromagnetic resonance

- GHz sources and detectors,
- Spintronics,
- Magnon-photon coupling is investigated, birth of spincavitronics promissing quantum computing applications.

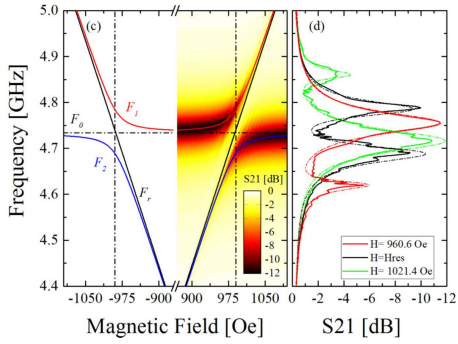

[1] L. Bai et al., Phys. Rev. Lett. **114**, 227201 (2015)
[2] V. Castel et al., Phys. Rev. B **96**, 064407 (2017)

Antiferromagnets and THz range.

- Frequency of antiferromagnetic resonances fall in the THz range.
- Wide variety of materials available.
- They do not require external magnetic field.
- Potential THz sources and detectors.
- High-frequency spintronics.
- However, state of an antiferromagnet is hardly detectable.
- Magnon-photon coupling is investigated in ferromagnets but not in antiferromagnets yet.

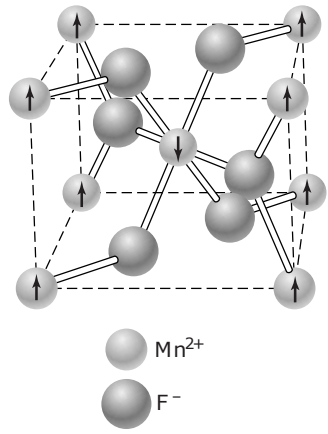

Antiferromagnetic resonance

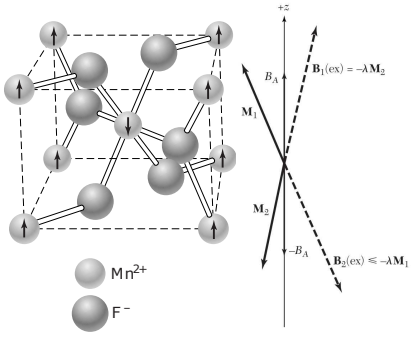

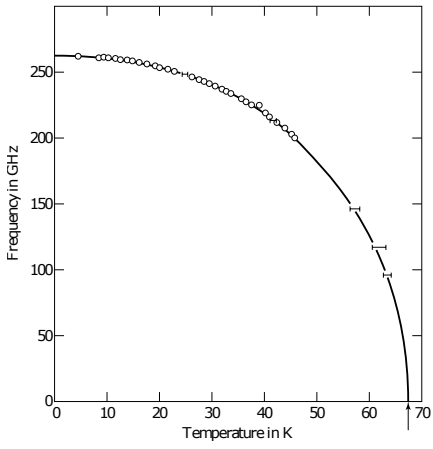

B_E – exchange field

B_A – anisotropy field

$\omega = \gamma\sqrt{B_A(B_A + 2B_E)} \approx \gamma\sqrt{2B_AB_E}$

Rare-earth ferrites

Dysprosium ferrite ($DyFeO_3$), yttrium ferrite ($YFeO_3$) and thulium ferrite ($TmFeO_3$)

- with high $T_N \approx 640$ K,
- spin-canting causing weak ferromagnetism,
- two spin-wave modes can be excited.

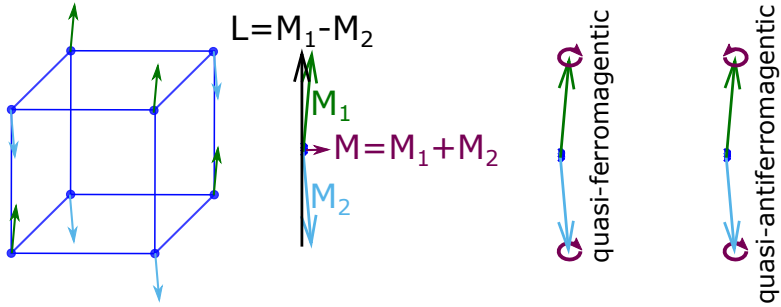

$$H = J_1 \sum_{(i,j)} \mathbf{S_i} \cdot \mathbf{S_j} + J_2 \sum_{(i,j)'} \mathbf{S_i} \cdot \mathbf{S_j} - D_2 \sum_{(i,j)} (-1)^{n_i} \mathbf{z}' \cdot (\mathbf{S_i} \times \mathbf{S_j})$$

Bismuth ferrite ($BiFeO_3$)

This compound is a high-temperature multiferroic:

- ferroelectric, with $T_C \approx 1100$ K,
- antiferromagnet, with $T_N = 643$ K,
- spin-cycloid structure with the period of 62 nm (222 lattice constants).

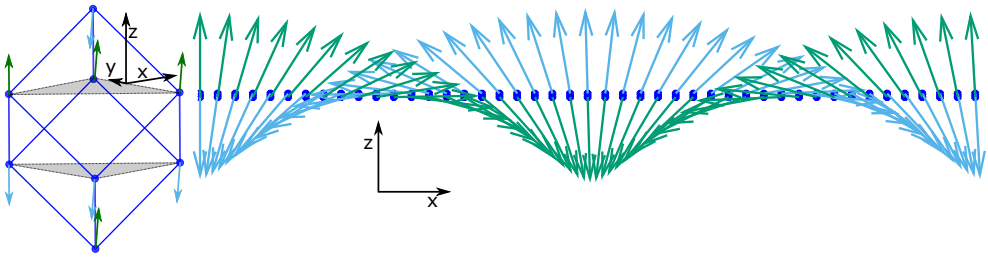

$$H = J_1 \sum_{(i,j)} \mathbf{S_i} \cdot \mathbf{S_j} + J_2 \sum_{(i,j)'} \mathbf{S_i} \cdot \mathbf{S_j} - D_1 \sum_{(i,j)} (\mathbf{z} \times \mathbf{e_{i,j}}/a) \cdot (\mathbf{S_i} \times \mathbf{S_j})$$

Spin-waves in bismuth ferrite

- Φ—modes oscillating in the cycloid plane. $\omega \sim k$
- Ψ—modes oscillating out of the cycloid plane. $\omega \sim \sqrt{1 + k^2}$
- Periodic magnetic structure folds spin-wave band structure.
- Few modes have nonzero intensity when excited by e-m radiation.

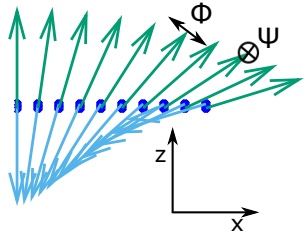

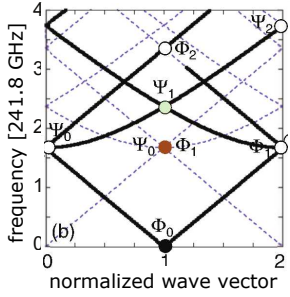

[1] R. S. Fishman et al., Phys. Rev. B **87**, 134416 (2013).

THz transmission with VNA

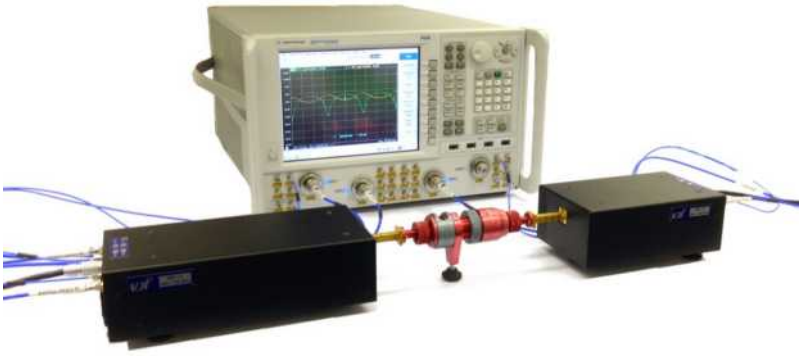

Standard procedure at room temperature:

- Calibrate.
- Measure.

THz transmission at high temperatures

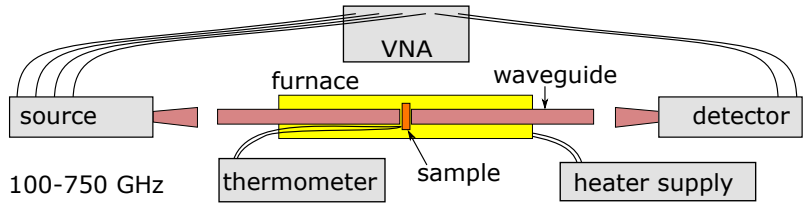

- The Néel temperature is at almost 400°C.
- Transmission drops exponentially with rising temperature.

Measurements

Frequency scans do not give clear results due to interference,

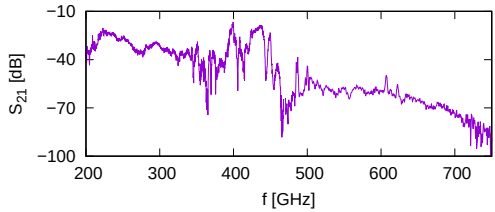

but temperature scans for fixed frequency do.

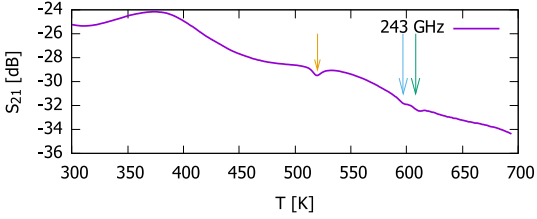

Temperature-differential spectra

$$\frac{\partial S_{21}}{\partial T}(f,T) = \Delta T^{-1}(S_{21}(f,T+\Delta T) - S_{21}(f,T))$$

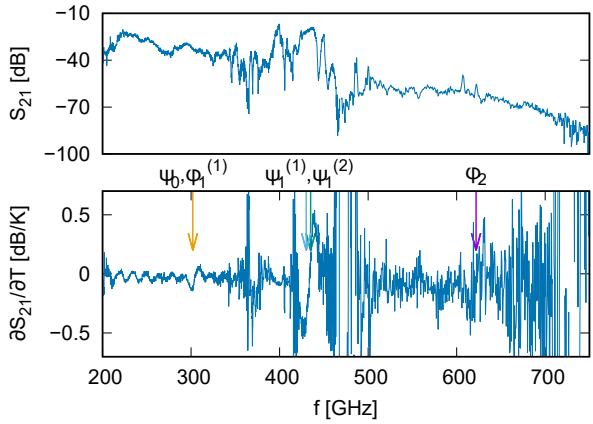

[1] M. Białek et al., Phys. Rev. B **97**, 054410 (2018).

Results in $TmFeO_3$

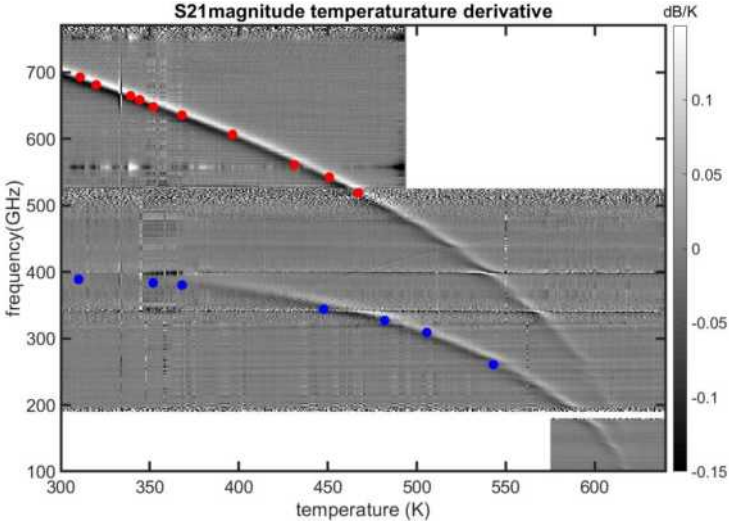

[1] A. M. Balbashov, High Frequency Processes in Magnetic Materials, pp. 56-98 (1995)

Results in $BiFeO_3$

- Four resonant lines can be traced.
- Interference in the sample slab depends on temperature.
- Resonant frequencies drop fast with temperature when approaching the Néel temperature.
- Oscillation of width of the $\Psi_0, \Phi_1^{(1)}$ resonance suggest interaction of spin-waves with the cavity modes.

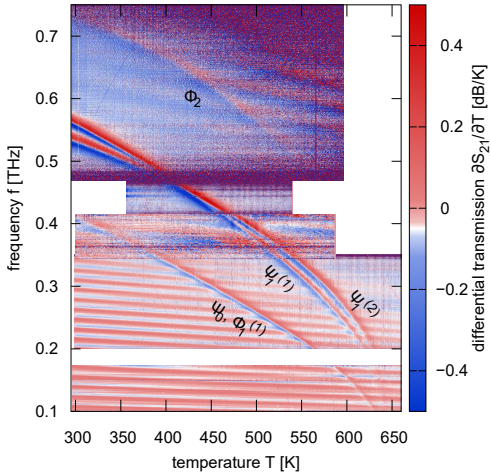

[1] M. Białek et al., Phys. Rev. B **97**, 054410 (2018).

Results in $BiFeO_3$

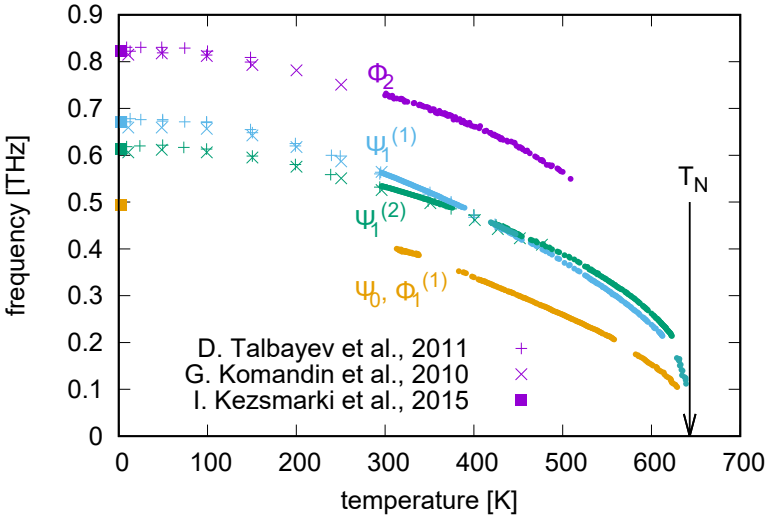

[1] M. Białek et al., Phys. Rev. B **97**, 054410 (2018).

Resonance width in BFO samples of different thicknesses

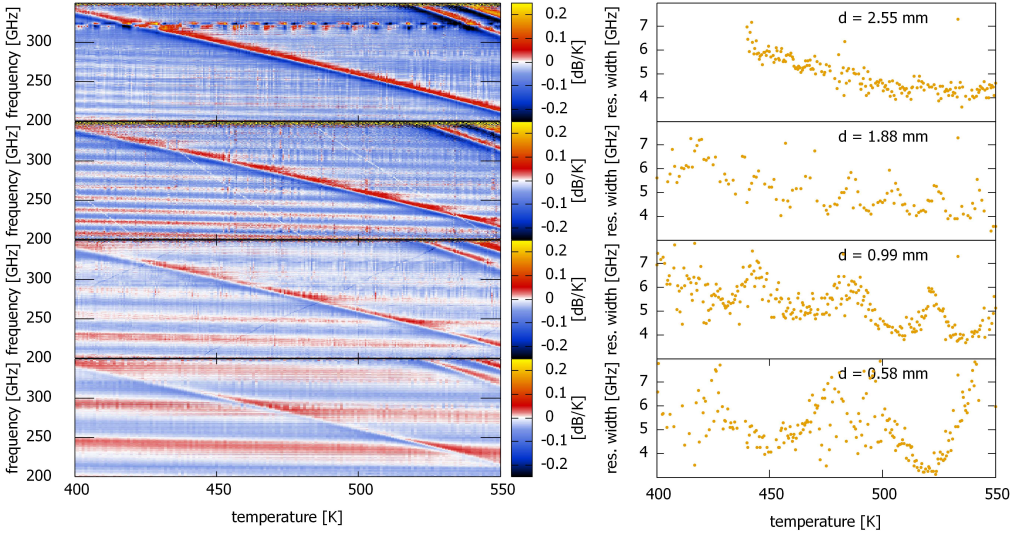

Transmission in electromagnetism

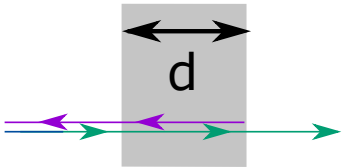

$$t(f,T) = \frac{(1-\rho^2)e^{ikd}}{1-\rho^2 e^{i2kd}}$$

$$k(f,T) = 2\pi f\sqrt{\epsilon\mu}/c \quad \rho(f,T) = \frac{\sqrt{\epsilon}-\sqrt{\mu}}{\sqrt{\epsilon}+\sqrt{\mu}}$$

$$\left\| \frac{\partial S_{21}}{\partial T}(f,T) \right\| = \frac{20}{\Delta T} log_{10} \left\| \frac{t(f,T+\Delta T)}{t(f,T)} \right\|$$

$$\epsilon(f,T) = \epsilon_{\text{inf}} + \sum_{l=1}^{M} \frac{\Delta\epsilon_l(T) f_l^2(T)}{f_l^2(T) - f^2 - if\gamma_l(T)}$$

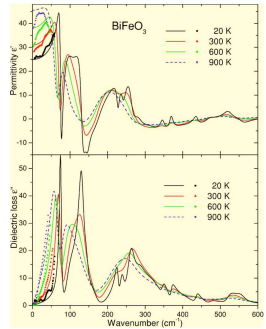

$$\mu(f,T) = 1$$

$$\epsilon(f,T) \approx \epsilon^{(0)} + af + b(T - T_0)$$

[1] M. Born and E. Wolf, Principles of Optics

Polaritons in electromagnetism

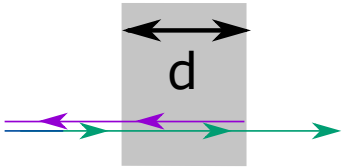

$$t(f,T) = \frac{(1-\rho^2)e^{ikd}}{1-\rho^2 e^{i2kd}}$$

$$k(f,T) = 2\pi f\sqrt{\epsilon\mu}/c \quad \rho(f,T) = \frac{\sqrt{\epsilon}-\sqrt{\mu}}{\sqrt{\epsilon}+\sqrt{\mu}}$$

$$\left\| \frac{\partial S_{21}}{\partial T}(f,T) \right\| = \frac{20}{\Delta T} log_{10} \left\| \frac{t(f,T+\Delta T)}{t(f,T)} \right\|$$

$$\epsilon(f,T) = \epsilon^{(0)} + af + b(T-T_0)$$

$$\mu(f,T) = 1 + \sum_{m=1}^{M} \frac{\Delta\mu_m(T) f_m^2(T)}{f_m^2(T) - f^2 - if\gamma_m(T)}$$

$$f_m(T) = f_m^0 \left(1 - \frac{T}{T_N}\right)^{\beta_m}$$

$$\gamma_m(T) = g_m^{T0}(1 + dg_T(T-T_0))$$

$$\Delta\mu_m(T) = \Delta\mu_m^{T0}(1 + dm_T(T-T_0))$$

[1] M. Born and E. Wolf, Principles of Optics

[2] D. L. Mills and E. Burstein, Rep. Prog. Phys. **37** 817 (1974)

Results in BFO and model fits

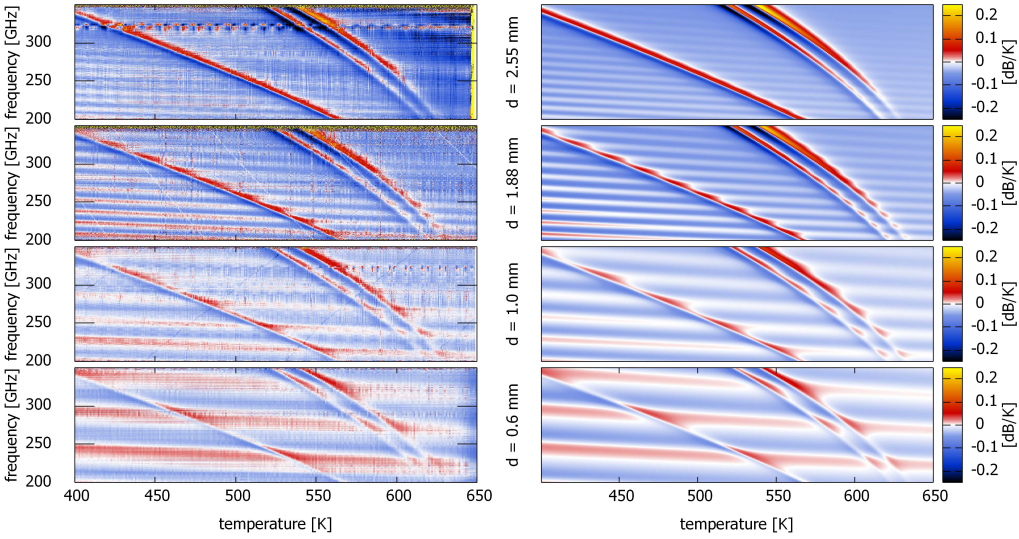

Microscopic model

$$f_{\pm} = \frac{1}{2}\left(f_c + f_m \pm \sqrt{(f_c - f_m)^2 + 4\kappa^2 f_c}\right)$$

$$\kappa\sqrt{f_c} = \frac{g_s\mu_B}{2h}B_0\sqrt{N} = \frac{g_s\mu_B}{2h}\sqrt{\frac{\mu_0 h}{2}}\rho\sqrt{f_c}$$

$$B_0 = \sqrt{\frac{\mu_0 h}{2}\frac{f_c}{V_c}}$$

$$N = \rho V_c$$

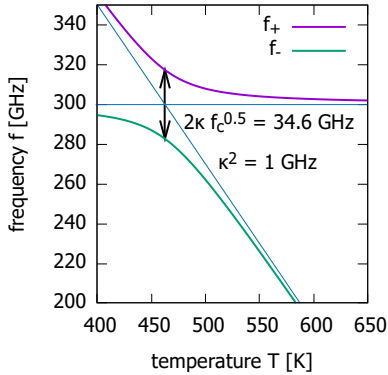

[1] H. Huebl, C. W. Zollitsch, J. Lotze, F. Hocke, M. Greifenstein, A. Marx, R. Gross, and S. T. B. Goennenwein, Phys. Rev. Lett. **111**, 127003 (2013).

BFO—microscopic model fit to 0.6-mm-thick sample

$$\kappa = \frac{g_s \mu_B}{2h} \sqrt{\frac{\mu_0 h}{2}} \rho$$

$$\rho \approx \frac{1}{22} \rho_{Fe}$$

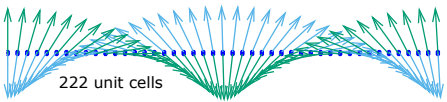

- Long period of the cycloid.
- Electromagnetic coupling.

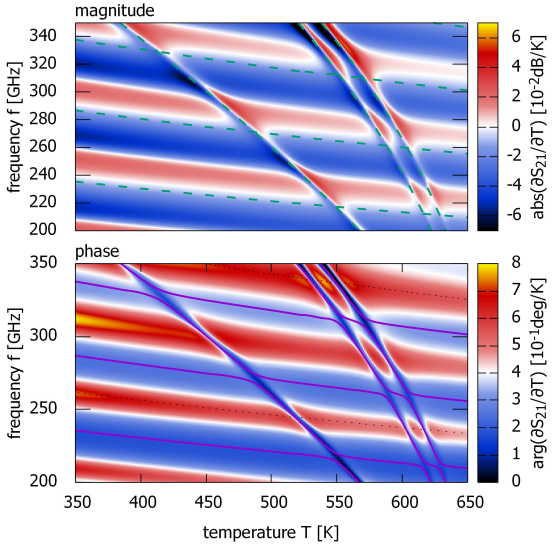

Results in DFO

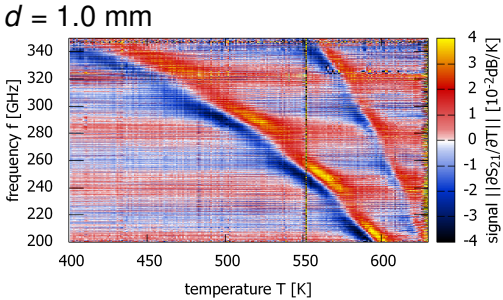

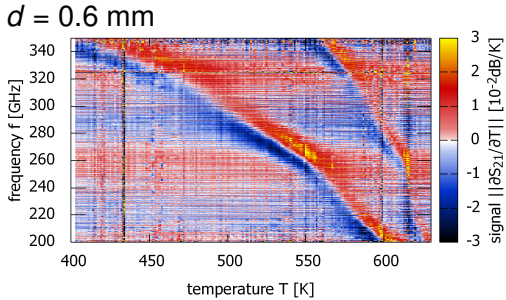

Results in DFO and model fits: magnitude

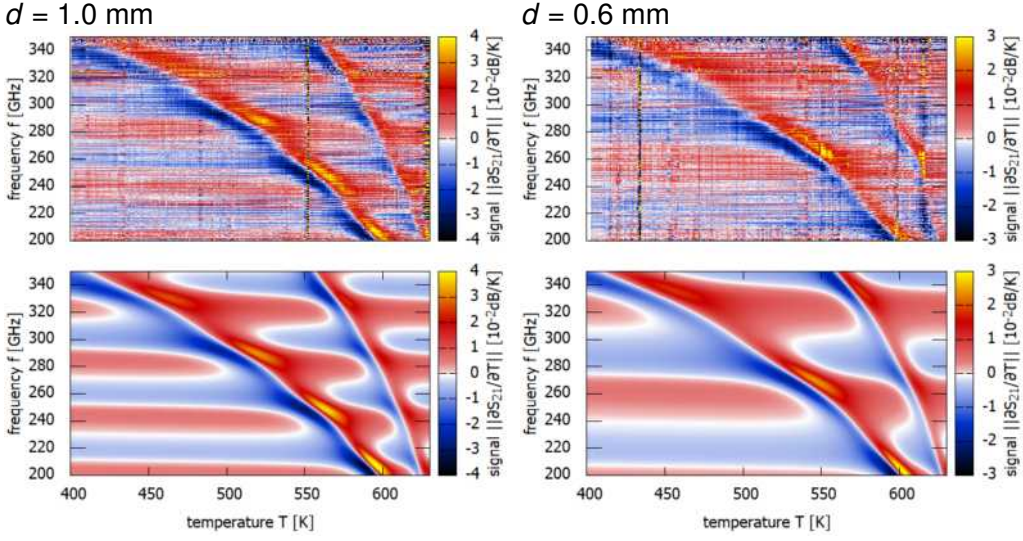

Results in DFO and model fits: phase

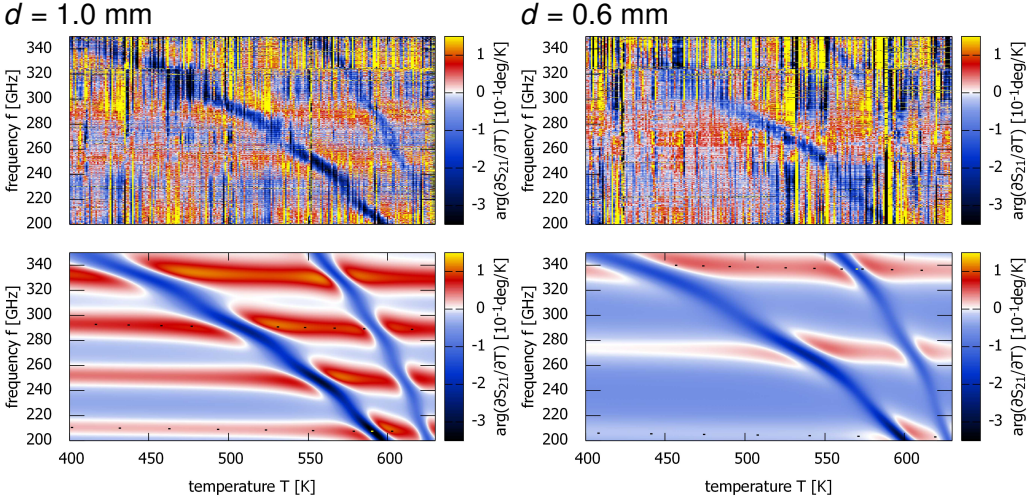

DFO: ϵ and μ

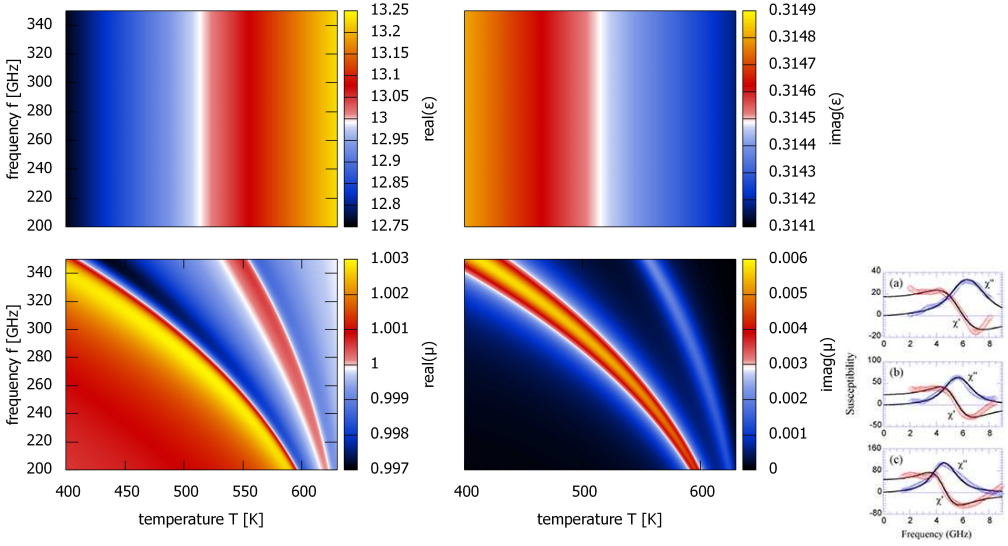

DFO—microscopic model fit to 1.0-mm-thick sample

$$\kappa = \frac{g_s \mu_B}{2h} \sqrt{\frac{\mu_0 h}{2} \rho}$$

$$\rho = \frac{1}{3} \rho_{Fe}$$

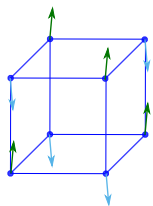

because 1/3 of magnetic moments is excited in a polycrystaline

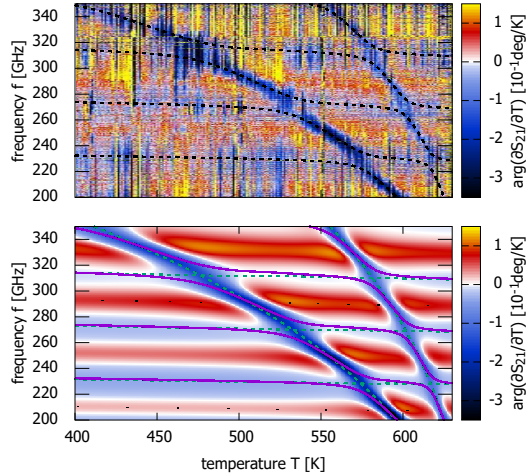

DFO—microscopic model fit to 1.0-mm-thick sample

$$\kappa = \frac{g_s \mu_B}{2h} \sqrt{\frac{\mu_0 h}{2}} \rho$$

$$\rho = \frac{1}{3} \rho_{Fe}$$

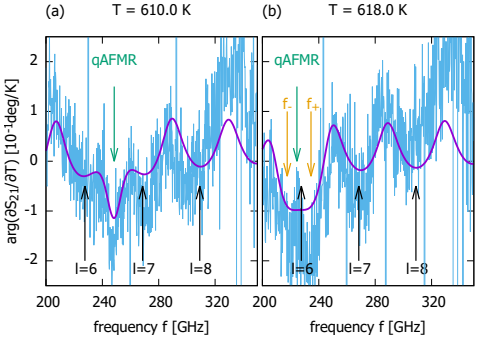

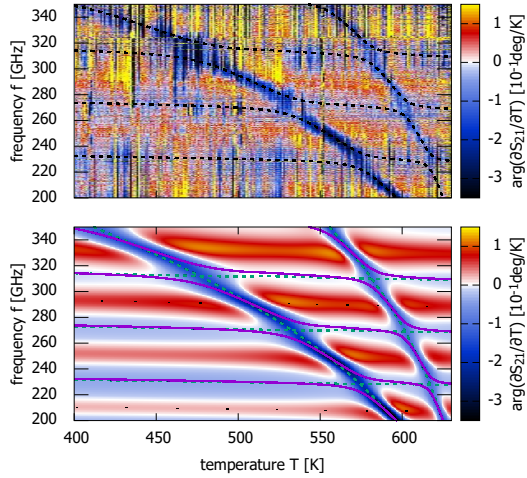

Magnetic field modulation

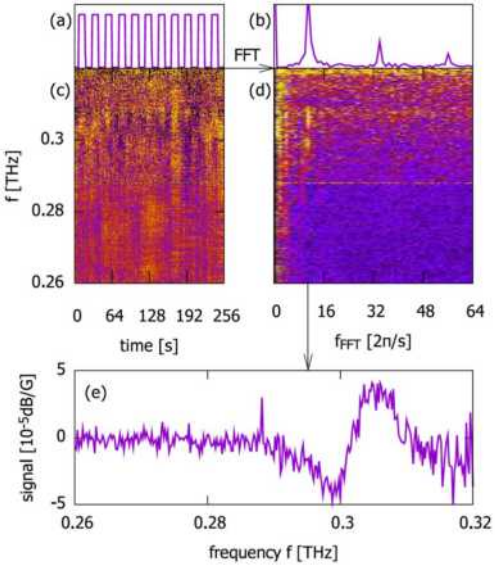

- Used when magnetic resonance is temperature-independent.
- Reveals very tiny signals.

DFO 0.6-mm-thick sample in magnetic field modulation

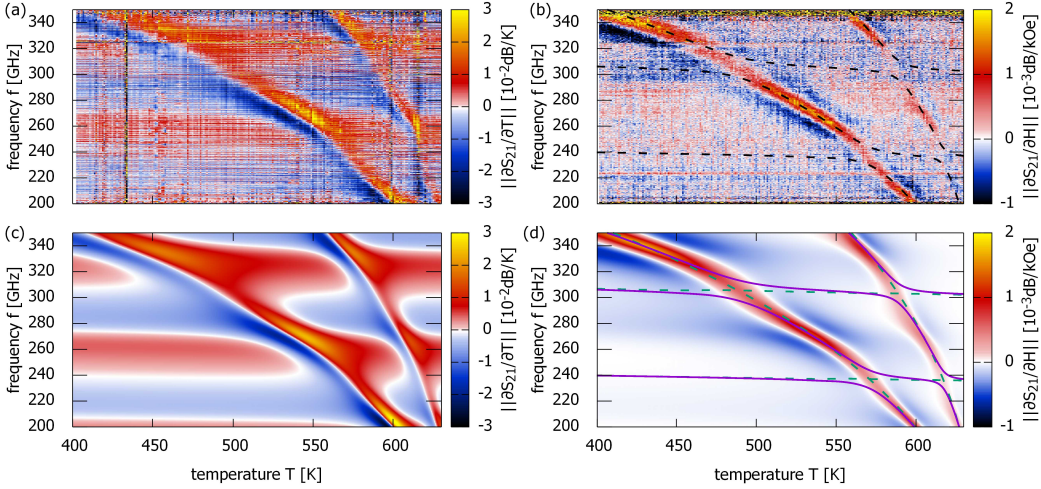

Yttrium ferrite single crystal in large optical cavities

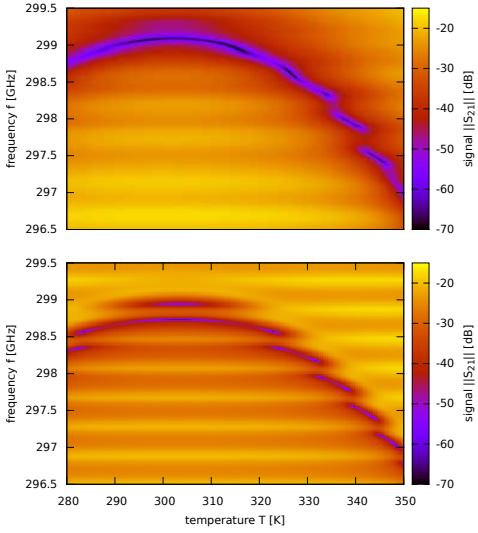

- The cavity is formed by dielectric mirrors about 40 cm apart.
- Tiny frequency scale of observed splitting.
- Anisotropic properties of the crystal are crucial.

Summary

- VNA detects THz antiferromagnetic resonances.
- Magnon-polaritons were observed in the THz range in antiferromagnets.
- Magnon-photon coupling was described using electromagnetism.
- The coupling strength was estimated using a microscopic model.

[1] M. Białek, A. Magrez and J-.Ph. Ansermet, Phys. Rev. B **101**, 024405 (2020)
[2] M. Białek, T. Ito, H. Rønnow and J-.Ph. Ansermet, Phys. Rev. B **99**, 064429 (2019).
[3] M. Białek, A. Murk, A. Magrez and J-.Ph. Ansermet, Phys. Rev. B **97**, 054410 (2018).